

# Poly(*N*-acryloylsarcosine methyl ester) Protein-Resistant Surfaces

D. O. H. Teare, W. C. E. Schofield, R. P. Garrod, and J. P. S. Badyal\*

Department of Chemistry, Science Laboratories, Durham University, Durham DH1 3LE, England, U.K.

Received: May 25, 2005; In Final Form: August 30, 2005

A new class of protein-resistant film based on *N*-substituted glycine derivatives is described. Pulsed plasma deposited poly(*N*-acryloylsarcosine methyl ester) coatings are shown to be resistant toward the adsorption of fibrinogen and lysozyme. Deposition and UV irradiation of the polymer through a masked grid are found to be effective ways for generating negative and positive image protein arrays, respectively, onto a range of different substrate materials.

## 1. Introduction

The forces which are understood to govern protein adsorption onto a solid surface comprise hydrogen bonding, hydrophobic, and electrostatic interactions.<sup>1</sup> Hydrogen bonds tend to form between polar groups contained in the protein and those present on the surface. Hydrophobic forces arise due to the formation of a water depletion zone at the interface between hydrophobic regions on a protein molecule and a hydrophobic substrate, while electrostatic interactions are associated with solvated charged groups on the protein surface and the solid substrate. Once absorbed onto a surface, a protein may either stay in its natural conformation, or denature (unfold), and such binding can be irreversible.<sup>2</sup> For instance, in the case of hydrophobic substrates, proteins usually unfold in order to maximize interactions with the surface.

Since the late 1980s there has been a growing interest in surfaces and coatings which resist bioadhesion (i.e., proteins, cells, and bacteria). The most widely studied systems have been based upon poly(ethylene oxide) (PEO)/poly(ethylene glycol) (PEG),<sup>3–6</sup> phospholipids,<sup>7</sup> polysaccharides,<sup>8–12</sup> and polyacrylamides.<sup>13,14</sup> As a general rule, surfaces which minimize protein adsorption prove to be resistant toward cell attachment and tissue culture growth.<sup>9,12</sup>

PEO/PEG surfaces are considered to be the benchmark performers for minimizing protein adhesion. The nonfouling character of PEO surfaces is attributed to the very high levels of polymer chain hydration as well as the conformational flexibility of the polymer.<sup>15,16</sup> A number of methods exist for making PEO surfaces; these include gold-,<sup>8,17</sup> silicon-,<sup>18</sup> silica-,<sup>19</sup> and diamond-based<sup>20</sup> self-assembled monolayers (SAMs), physisorption<sup>21,22</sup> chemisorption,<sup>17,23,24</sup> surface-initiated polymerization,<sup>22</sup> plasma-initiated grafting,<sup>25</sup> covalent grafting onto a plasma polymer,<sup>26</sup> and plasma polymerization.<sup>27,28</sup> A PEO-mimicking thiol-functionalized polyester with ether side chains SAM on gold has also been shown to display minimal protein adsorption characteristics.<sup>29</sup> Many of these systems have intrinsic disadvantages: PEO suffers from a susceptibility toward oxidative degradation and chain cleavage in aqueous environments<sup>30</sup> (PEO coatings can degrade and lose their bioinertness after several days of immersion in buffer<sup>12,31</sup>). Alkanethiol-gold-based SAMs (which comprise the majority of systems studied so far) have an additional disadvantage in that the thiolate linkages

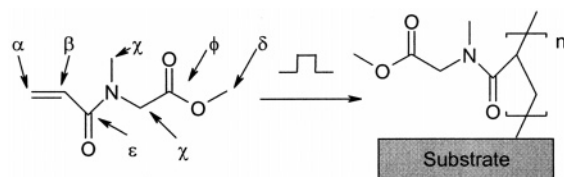
(Au–SR) are vulnerable to oxidation and desorption from the gold surface, leading to a complete loss of the protein-resistant properties.<sup>32</sup>

Phospholipids are another extensively studied class of molecules capable of rendering surfaces protein resistant. These biomimetic surfaces resemble the outer lipid membrane surface of erythrocytes, and as such they are nonthrombogenic.<sup>7</sup> In particular, phosphorylcholine (the headgroup of lecithin<sup>1</sup>) based surfaces have been shown to improve biocompatibility.<sup>33</sup> The protein resistance behavior of phosphorylcholine surfaces can be attributed to the very high levels of hydration of the zwitterionic headgroup; these positive and negative charges render the surface neutral over a large pH range.<sup>34</sup> This hydration layer ensures that proteins which come into contact with the surface do so reversibly and without deformation.<sup>35</sup> Many of the methods employed to produce phosphorylcholine surfaces rely on the ability of these amphiphilic molecules to self-assemble as planar supported lipid bilayers<sup>36</sup> (or multilayers). This has been achieved by spin coating,<sup>37</sup> Langmuir–Blodgett deposition,<sup>38</sup> and liposome adsorption.<sup>39</sup> However, a major drawback encountered with most of these systems is that they are reliant upon weak van der Waals interactions (the phosphorylcholine molecules themselves being only weakly associated with each other and to the underlying substrate, thereby compromising the overall bulk physical properties of the material<sup>33</sup>). Attempts aimed at improving the binding of phosphorylcholine-based films have included grafting to plasma-irradiated surfaces,<sup>40</sup> forming SAMs of phosphorylcholine-terminated alkanethiols onto gold,<sup>9,41</sup> cross-linking the phosphorylcholine chains via diene groups in the alkyl chains,<sup>36</sup> and copolymerizing phosphorylcholine methacrylates with other monomers.<sup>35,42</sup>

Saccharide groups are also renowned for their protein-resistant behavior. In a similar mode d'emploi to PEO/PEG and phospholipids, these hydrophilic surfaces are highly hydrated and thus render the substrate protein resistant. For instance, dextran is reported to be protein resistant and limits the adhesion and spreading of cells,<sup>43</sup> although absolute protein rejection is not observed.<sup>44,45</sup> Alkanethiol-based saccharide SAMs which have displayed protein resistance comparable to PEO, include methylated sorbitol<sup>8–11</sup> and mannitol.<sup>12</sup> The latter is capable of sustaining protein-resistant behavior for much longer periods of time compared to PEO-based SAMs (thus overcoming one of the principal disadvantages of PEO).

\* To whom correspondence should be addressed.

### SCHEME 1. Pulsed Plasma Polymerization of *N*-Acryloylsarcosine Methyl Ester



Polyacrylamides are another category of protein-resistant surface. In particular, the thermoresponsive polymer poly(*N*-isopropylacrylamide) behaves as a protein-resistant material *below* its lower critical solution temperature (LCST), and switches to being protein absorbent *above* its LCST.<sup>13,14</sup> A main disadvantage in this case is that it absorbs protein at body temperature.<sup>46</sup>

Other surfaces that have been found to exhibit protein resistance include tripropylsulfoxide-terminated alkanethiol SAMs<sup>47</sup> and elastin-like polypeptide coatings.<sup>22,48</sup> Lately, there has been an interest in various alternative protein-resistant alkanethiol-gold SAMs based on kosmotropes (molecules that exclude themselves from the protein-water interface<sup>11</sup>) such as polyols, betaine,<sup>42,49</sup> taurine, trimethylamine-*N*-oxide, dimethyl acetamide, dimethyl sulfoxide, and hexamethylphosphoramide.

Finally, there is an alternative strategy where absorption of serum albumin onto a surface can lead to the suppression of protein adsorption.<sup>50,51</sup> However, this method is not particularly robust, and adsorbed proteins are vulnerable to eventual displacement by more surface active proteins due to the Vroman effect.<sup>52</sup>

In this article we report the fabrication of protein-resistant surfaces by the polymerization of *N*-acryloylsarcosine methyl ester (e.g., by pulsed plasma deposition), Scheme 1. This precursor is of interest because it obeys the set of four molecular criteria postulated by Whitesides for protein resistance;<sup>10</sup> these being the presence of (i) polar functional groups, (ii) hydrogen bond accepting groups, (iii) the absence of hydrogen bond donating groups, and (iv) no net charge. Previously, alkanethiol-terminated gold SAMs of sarcosine-based polypeptides have been shown to exhibit good protein-resistant properties.<sup>9</sup> However, SAM systems are known to suffer from being substrate specific and tend to be unstable as a consequence of their thiolate groups being susceptible toward oxidation and desorption from the gold surface.<sup>32</sup> Alternative *N*-substituted glycine (peptoid) oligomers coupled to a short functional peptide domain for surface attachment are limited to physisorption.<sup>53</sup> These limitations are overcome by adopting an acrylamide form of sarcosine for polymerization to produce a protein-resistant film. The merits of pulsed plasmachemical deposition are that it is a straightforward and effective method for functionalizing solid surfaces (single-step, solventless, chemical attachment, and substrate-independent). This constitutes the generation of active sites (predominantly radicals) at the surface and in the electrical discharge during the duty cycle on-period, followed by conventional polymerization reaction pathways proceeding during each extinction period. Typical time scales are of the order of microseconds and milliseconds, respectively. The level of surface functionalization can be tailored by simply preprogramming the pulsed plasma duty cycle. Functional films containing high levels of anhydride,<sup>54</sup> carboxylic acid,<sup>55</sup> cyano,<sup>56</sup> epoxide,<sup>57</sup> hydroxyl,<sup>58</sup> furfuryl,<sup>59</sup> perfluoroalkyl,<sup>60</sup> perfluoromethylene,<sup>61</sup> or trifluoromethyl<sup>62</sup> groups have been successfully prepared in the past using this methodology.

## 2. Experimental Section

*N*-Acryloylsarcosine methyl ester monomer (97%, Lancaster, liquid at room temperature and boiling point of 96°C) was loaded into a sealable glass tube and further purified using multiple freeze-pump-thaw cycles. Plasma polymerization was carried out in a cylindrical glass reactor (4.5 cm diameter, 460 cm<sup>3</sup> volume,  $2 \times 10^{-3}$  mbar base pressure, and  $1.4 \times 10^{-9}$  mol s<sup>-1</sup> leak rate), surrounded by a copper coil (4 mm diameter, 10 turns, located 15 cm away from the precursor inlet) and connected to a 13.56 MHz radio frequency (rf) power supply via an L-C matching network. The reactor was located inside a temperature-controlled oven (set at 40 °C for sufficient monomer vapor pressure) and a Faraday cage (to prevent leakage of rf radiation). A 30 L min<sup>-1</sup> rotary pump attached to a liquid nitrogen cold trap was used to evacuate the plasma chamber. System pressure was monitored with a Pirani gauge. All fittings were grease free. During pulsed plasma deposition, the rf power source was triggered by a signal generator and the pulse shape was monitored with an oscilloscope. Prior to each experiment, the apparatus was scrubbed with detergent, rinsed with propan-2-ol, and oven dried. Further cleaning entailed running a continuous wave air plasma at 0.2 mbar pressure and 40 W power for 20 min. Next, silicon wafers, gold chips, or cut polystyrene squares (15 mm × 15 mm) were inserted into the reactor, and the system pumped down to base pressure. A continuous flow of *N*-acryloylsarcosine methyl ester vapor was introduced into the chamber at a pressure of 0.1 mbar and 40 °C for 5 min prior to plasma ignition. The optimum pulsed plasma duty cycle corresponded to 30 W peak power ( $P_p$ ) continuous wave bursts lasting 20 μs ( $t_{on}$ ) followed by an off-period ( $t_{off}$ ) set to 5 ms. Once deposition was completed, the rf power was switched off, and the monomer was allowed to continue to purge through the system for a further 5 min prior to evacuating to base pressure and venting to atmosphere.

A spectrophotometer (nkd-6000, Aquila Instruments Ltd.) was used to measure plasma polymer film thickness and deposition rate. The obtained transmittance-reflectance curves (350–1000 nm wavelength range) were fitted to a Cauchy model using a modified Levenberg-Marquardt algorithm.<sup>63</sup>

Contact angle analysis of the plasma-deposited *N*-acryloylsarcosine methyl ester films was carried out with a video capture system (ASE Products, model VCA2500XE) using 2.0 μL droplets of deionized water.

X-ray photoelectron spectroscopy (XPS) was undertaken using an electron spectrometer (VG ESCALAB MK II) equipped with a nonmonochromated Mg Kα<sub>1,2</sub> X-ray source (1253.6 eV) and a concentric hemispherical analyzer. Photoemitted electrons were collected at a takeoff angle of 30° from the substrate normal, with electron detection in the constant analyzer energy mode (CAE, pass energy = 20 eV). The XPS spectra were charge referenced to the C(1s) peak at 285.0 eV and fitted with a linear background and equal full width at half-maximum Gaussian components<sup>64</sup> using Marquardt minimization computer software. Instrument sensitivity (multiplication) factors derived from chemical standards were taken as being C(1s):O(1s):N(1s) = 1.00:0.36:0.57.

Surface infrared spectroscopy of plasma polymer coated gold slides was performed using an FTIR spectrometer (Perkin-Elmer, model Spectrum One) equipped with a liquid nitrogen cooled MCT detector operating at 4 cm<sup>-1</sup> resolution over the 700–4000 cm<sup>-1</sup> range. A reflection absorption accessory (RAIRS, Specac) and a KRS-5 p-polarizer were fitted to the instrument, with the reflection angle set to 80°.

Surface plasmon resonance (SPR) protein adsorption studies entailed plasma deposition of 25 nm thick poly(*N*-acryloylsarcosine methyl ester) films onto a gold sensor chip (Biacore) and monitoring protein adsorption using a biosensor SPR system (Biacore 1000 upgrade). Fibrinogen (from bovine plasma, Sigma) and lysozyme (egg white, Sigma) proteins were screened. Fibrinogen is a large protein which interacts with platelets during blood clotting; it is a good example of a “sticky protein”.<sup>65</sup> Lysozyme is smaller and positively charged<sup>66</sup> under the experimental conditions used and is often employed as a model protein to study electrostatic adsorption.<sup>67</sup> The experimental protocol for measuring protein adsorption entailed first ensuring a clean surface by flowing a 40 mM in phosphate buffered saline solution of sodium dodecyl sulfate (+99%, Sigma) over the surface for 3 min followed by flushing with phosphate-buffered saline (pH 7.4) for 10 min. At this stage, the absence of detergent associating with the surface was confirmed by XPS. Next, the protein solution (1 mg mL<sup>-1</sup> in phosphate-buffered saline, pH 7.4) was passed over the surface for 30 min. Finally, phosphate-buffered saline was flushed through the system for 10 min in order to dislodge any loosely bound proteins. The flow rate for all SPR experiments was set at 10  $\mu$ L min<sup>-1</sup>. In all cases, the buffer was degassed and filtered using a 200 nm cellulose nitrate filter (Whatman) prior to use.

Alexa-fluor 633 goat anti-mouse immunoglobulin (IgG, 2 mg mL<sup>-1</sup> in phosphate-buffered saline, Molecular Probes) further diluted to a concentration of 250  $\mu$ g mL<sup>-1</sup> in phosphate-buffered saline was employed as a fluorescent marker for mapping patterned arrays of pulsed plasma deposited poly(*N*-acryloylsarcosine methyl ester) films by fluorescent microscopy. Negative image protein arrays were created by embossing nickel grids (2000 mesh, 7.5  $\mu$ m holes with 5  $\mu$ m bars, Agar Scientific) into polystyrene plates using a weight of 4 tons for 10 s, followed by pulsed plasma deposition of poly(*N*-acryloylsarcosine methyl ester). The nickel grid was then lifted off from the polystyrene substrate to leave behind a well-defined array of plasma polymer. Positive image protein arrays were created by pulsed plasma depositing poly(*N*-acryloylsarcosine methyl ester) films onto a blank polystyrene chip and then irradiating through a nickel mask (2000 mesh, 7.5  $\mu$ m holes with 5  $\mu$ m bars, Agar Scientific) using a wide band HgXe UV source arc-lamp (Oriol model 6136) operating at a power of 0.3 W cm<sup>-1</sup> for 40 min. This gave rise to the localized photodegradation of the protein-resistant surface functionality. All patterned chips were subsequently immersed into a 250  $\mu$ g mL<sup>-1</sup> solution of Alexa-fluor 633 IgG in phosphate-buffered saline for 60 min. This was followed by successive rinses in phosphate-buffered saline, 50% phosphate-buffered saline diluted with deionized water, and finally twice with deionized water prior to fluorescent microscopy analysis. A Raman microscope system (LABRAM, Jobin Yvon) was used to collect a two-dimensional fluorescent map of the Alexa-fluor 633 IgG protein patterned surfaces. This entailed focusing an attenuated 633 nm He–Ne laser beam (20 mW) onto the sample using a microscope objective (50 $\times$ ) and the corresponding fluorescence signal collected through the same objective via a back-scattering configuration in combination with a cooled CCD detector. The diffraction grating was set at 300 grooves mm<sup>-1</sup> with the laser filter at 100% transmission. The sample was mounted onto a computerized X–Y translational mapping stage and the surface rastered (50  $\mu$ m  $\times$  50  $\mu$ m) using a 1  $\mu$ m step size.

### 3. Results

The stoichiometry of the plasma deposited poly(*N*-acryloylsarcosine methyl ester) films was determined by XPS, Table 1.

**TABLE 1: XPS Elemental Analysis and Water Contact Angles for Plasma-Deposited Poly(*N*-acryloylsarcosine methyl ester)<sup>a</sup>**

conditions	XPS			contact angle/deg
	% C	% N	% O	
continuous wave	72 $\pm$ 0.6	9 $\pm$ 0.1	19 $\pm$ 0.5	41 $\pm$ 1.7
pulsed	66 $\pm$ 0.5	9 $\pm$ 0.1	25 $\pm$ 0.6	44 $\pm$ 0.9
theoretical	64	9	27	N/A

<sup>a</sup>  $P_p$  = 30 W (continuous wave and pulsed),  $t_{on}$  = 20  $\mu$ s, and  $t_{off}$  = 5 ms).

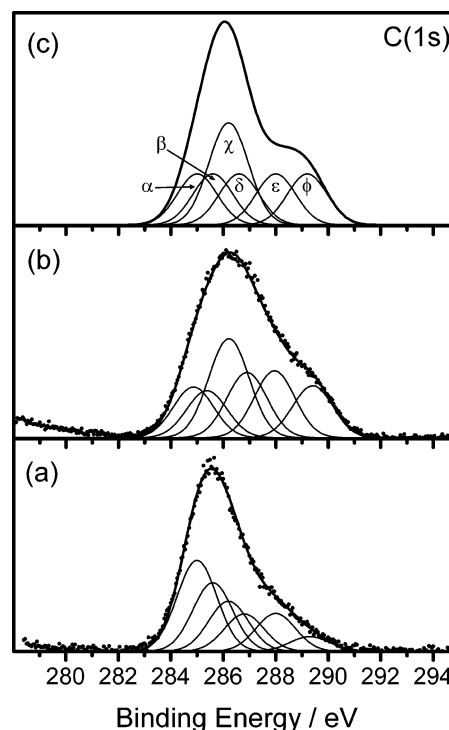


**Figure 1.** XPS C(1s) envelope of poly(*N*-acryloylsarcosine methyl ester): (a) 30 W continuous wave plasma deposited; (b) pulsed plasma deposited ( $P_p$  = 30 W,  $t_{on}$  = 20  $\mu$ s,  $t_{off}$  = 5 ms); and (c) theoretically predicted.

Pulsing the plasma at a duty cycle of  $P_p$  = 30 W,  $t_{on}$  = 20  $\mu$ s, and  $t_{off}$  = 5 ms produced films most resembling the theoretically predicted structure, Scheme 1. The absence of any Si(2p) XPS signal from the underlying silicon or gold substrates verified pinhole-free film thicknesses exceeding the XPS sampling depth (2–5 nm).<sup>68</sup> The XPS C(1s) envelope can be fitted to six carbon environments: hydrocarbon ( $C_xH_y$  = 285.0 eV,  $\alpha$ ), carbon adjacent to a carbonyl group ( $C-C=O$  = 285.7 eV,  $\beta$ ), carbon attached to nitrogen ( $C-N$  = 286.2 eV,  $\gamma$ ), carbon attached to oxygen ( $C-O$  = 286.6 eV,  $\delta$ ), carbon attached to nitrogen and oxygen ( $N-C=O$  = 288 eV,  $\epsilon$ ), and carbon attached to two oxygens ( $O-C=O$  = 289.3 eV,  $\phi$ ), Figure 1 and Scheme 1. Thirty watt continuous wave plasma deposited *N*-acryloylsarcosine methyl ester films display a high level of disruption of monomer structure as evident from the elemental composition and the distribution of C(1s) components, Table 1 and Figure 1. Much better structural retention was achieved during low duty cycle pulsed plasma deposition.

Structural retention for the pulsed plasma deposited poly(*N*-acryloylsarcosine methyl ester) films was also authenticated by infrared spectroscopy, Figure 2. Characteristic absorption bands include 1749 cm<sup>-1</sup> (ester carbonyl), 1653 cm<sup>-1</sup> (amide I), and 1212 cm<sup>-1</sup> (ester C–O). The carbon–carbon double bond absorption at 1615 cm<sup>-1</sup> associated with the monomer is not



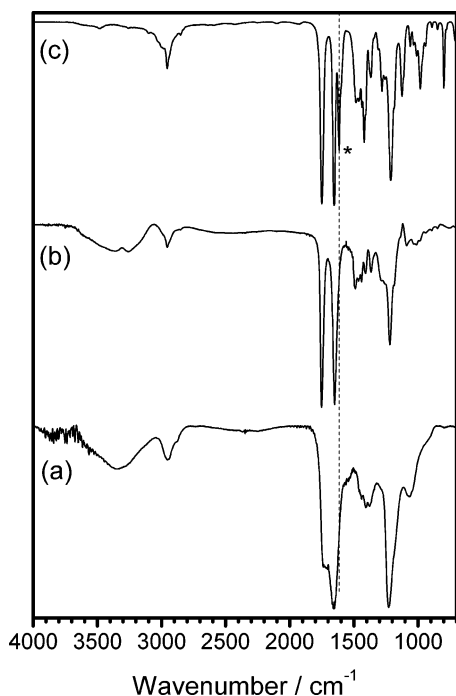


**Figure 2.** FTIR spectra of (a) 30 W continuous wave plasma polymerized *N*-acryloylsarcosine methyl ester, (b) pulsed plasma ( $P_p = 30$  W,  $t_{on} = 20$   $\mu$ s,  $t_{off} = 5$  ms) polymerized *N*-acryloylsarcosine methyl ester, and (c) *N*-acryloylsarcosine methyl ester monomer. (Asterisk denotes carbon-carbon double bond in precursor.)

present in any of the plasma deposited films, thus indicating complete polymerization of the precursor. Thirty watt continuous wave plasma deposition conditions yielded broad infrared absorption features, which can be taken as being symptomatic of a loss of monomer structural integrity. The low duty cycle pulsed plasma deposited film ( $P_p = 30$  W,  $t_{on} = 20$   $\mu$ s, and  $t_{off} = 5$  ms) displays much better resolved absorption bands matching those seen for the monomer (apart from the polymerizable carbon-carbon double bond stretch at  $1615$   $\text{cm}^{-1}$ ), thereby confirming a high degree of structural retention.

SPR analysis of fibrinogen and lysozyme adsorption onto 25 nm thick pulsed plasma deposited poly(*N*-acryloylsarcosine methyl ester) films ( $P_p = 30$  W,  $t_{on} = 20$   $\mu$ s, and  $t_{off} = 5$  ms) displayed excellent resistance toward protein adsorption, Figure 3. The films remained protein resistant at body temperature (i.e.,  $36$   $^{\circ}\text{C}$ ). In contrast, continuous wave plasma deposition conditions gave rise to approximately 2 orders of magnitude greater protein adsorption. UV irradiation of the pulsed plasma deposited poly(*N*-acryloylsarcosine methyl ester) for 40 min was sufficient to change the previously protein-resistant films to being as protein receptive as the continuous wave film. A range of oxidized surface functionalities had been created during UV irradiation (as observed by XPS).

SPR analysis of the adsorption of the fluorescent marker Alexa-fluor 633 IgG protein independently confirmed the good protein-resistance properties of the pulsed plasma deposited poly(*N*-acryloylsarcosine methyl ester) films, Figure 3. Fluorescence microscopy of an embossed array of pulsed plasma deposited poly(*N*-acryloylsarcosine methyl ester) following the adsorption of Alexa-fluor 633 IgG protein (negative image) showed clear contrast in signal intensity between the regions of plasma polymer (dark squares) and the uncoated polystyrene (bright grid), Figure 4. Whereas fluorescence microscopy of the UV-patterned pulsed plasma deposited poly(*N*-acryloylsarcosine methyl ester) array after exposure to Alexa-fluor 633 IgG protein

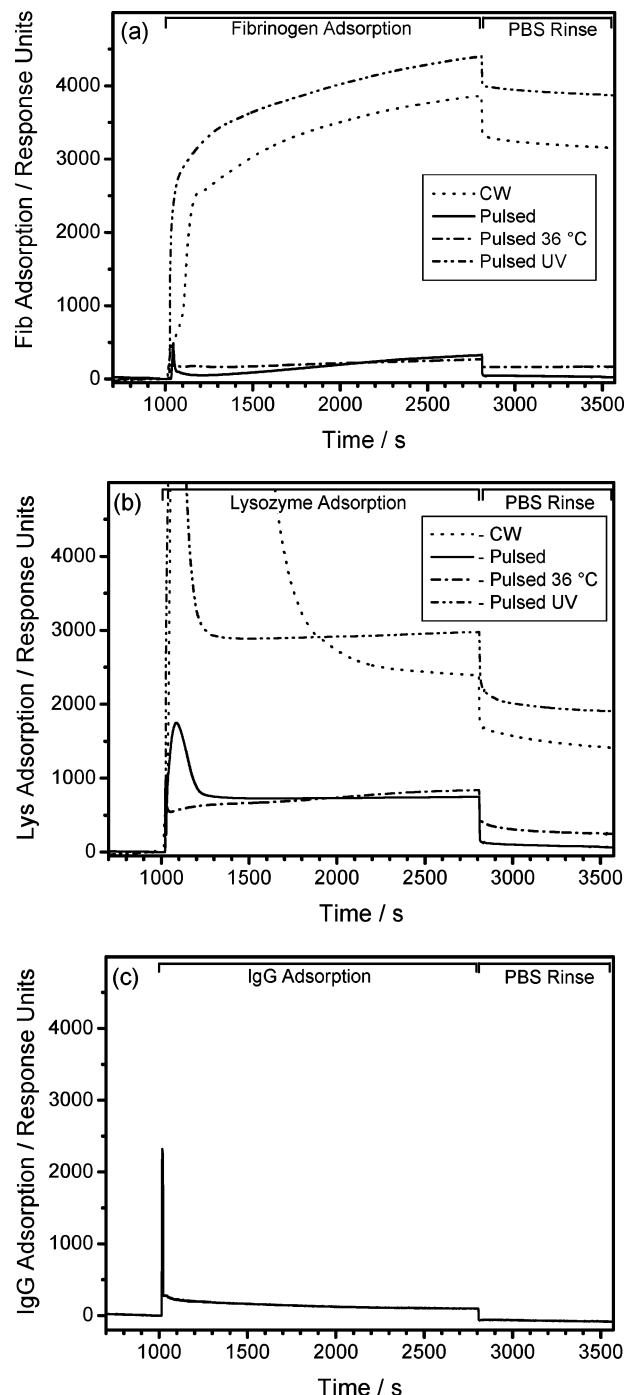


**Figure 3.** SPR of protein adsorption onto plasma polymerized *N*-acryloylsarcosine methyl ester films: (a) fibrinogen; (b) lysozyme; and (c) Alexa-fluor 633 IgG. ( $P_p = 30$  W (CW and pulsed),  $t_{on} = 20$   $\mu$ s, and  $t_{off} = 5$  ms.)

(positive image) only displayed signal intensity corresponding to UV exposure (bright squares) and not from the unexposed areas (dark grid).

#### 4. Discussion

Proteins in aqueous solution present hydrophilic groups at the protein-water interface, and any of these interfacial functionalities which are charged will attract an electric double layer of ions from the surrounding solution to screen the charge.<sup>69,70</sup> Along with these counterions a sheath of structured water molecules surrounding the protein will exist.<sup>71</sup> Likewise, a hydrophilic molecule such as protein-resistant PEO, phos-

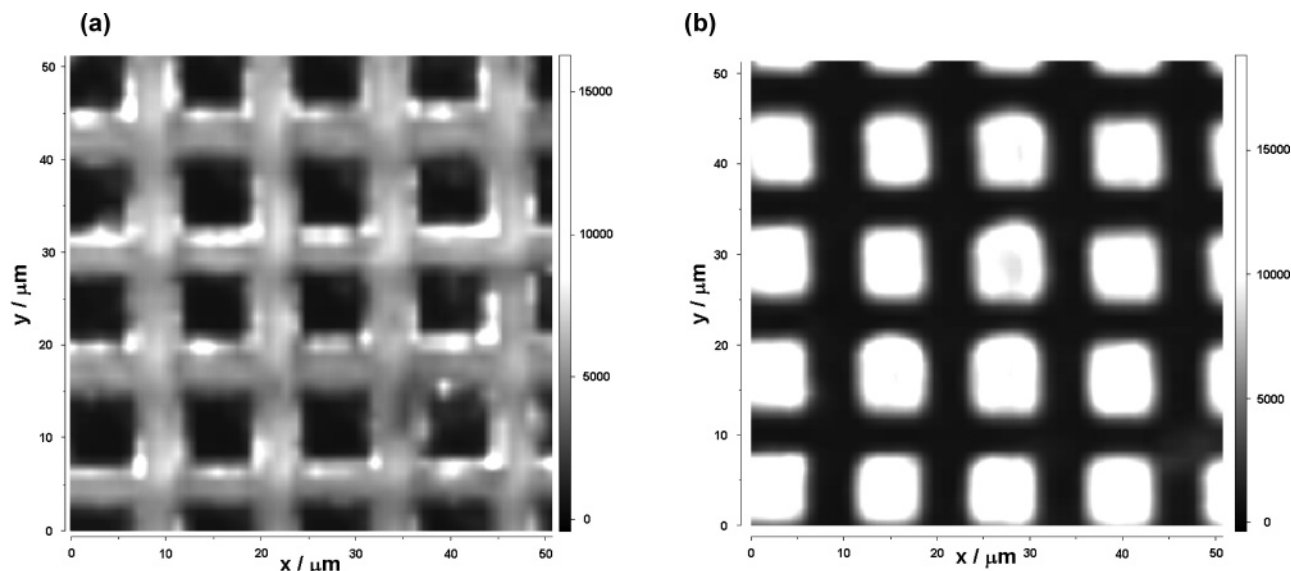


**Figure 4.** Fluorescence micrographs of pulsed plasma deposited poly(*N*-acryloylsarcosine methyl ester) arrays following immersion in Alexa-fluor 633 IgG/PBS solution: (a) embossed pattern (negative image); and (b) UV exposed pattern (positive image). ( $P_p = 30$  W,  $t_{on} = 20$   $\mu$ s, and  $t_{off} = 5$  ms.)

phorylcholine, or zwitterionic sulfobetaine will possess a similar surrounding sheath of ordered water molecules, as verified by Raman spectroscopy.<sup>72,73</sup> These protein-resistant moieties are understood to disrupt the ordering of water molecules in the domain local to a protein significantly less than non-protein-resistant substrates (such as poly(hydroxyethyl methacrylate),<sup>74</sup> sodium poly(ethylenesulfonate), and poly-L-lysine<sup>72</sup>). Thus in the former case, any long-range attractive forces between the protein and the surface are insufficient to overcome the steric repulsion encountered when the structured water interface around the protein and the surface try to overlap, and hence the surface is rendered protein resistant; i.e., it has an excluded volume.<sup>1</sup> However, this explanation alone is insufficient to describe protein resistance; other factors such as the packing, alignment, and flexibility of the surface molecules must also be taken into account.

Pulsed plasma deposited poly(*N*-acryloylsarcosine methyl ester) is hydrophilic with a contact angle of  $44 \pm 1.7^\circ$ , Table 1. This hydrophilicity stems from the terminal ester group and the polymer backbone amide linkages. Furthermore, the polymer does not contain any groups with hydrogen-bond-donating capacity; i.e., it obeys the set of four molecular criteria postulated by Whitesides for protein resistance.<sup>10</sup> Therefore it seems highly probable that the hydrated surface of poly(*N*-acryloylsarcosine methyl ester) films forms an exclusive volume to proteins that renders it protein resistant.

Tests in our laboratory have shown that the long-term protein resistance of the poly(*N*-acryloylsarcosine) surface does not deteriorate over 6 months. The plasma polymer is not susceptible toward oxidative degradation when placed in air (20 °C), phosphate-buffered saline solution (pH 7.4), or fibrinogen and lysozyme protein solutions, thus avoiding the disadvantage associated with PEO films. Furthermore, it benefits in that—unlike poly(*N*-isopropylacrylamide)—this polymer remains protein resistant at body temperature (36 °C). In the case of pulsed plasmachemical deposition, the coating is also substrate independent, giving applicability to diverse uses such as protein-resistant biomaterials and proteomics chips. The coating has been applied to gold, glass, silicon, polystyrene microspheres, and polymer nonwovens.

Alternative methods for functionalizing a surface using protein-resistant *N*-acryloylsarcosine methyl ester or other

sarcosine-based monomers include atomized spray plasma deposition,<sup>75</sup> grafting by preirradiation of a surface with ionizing radiation<sup>76</sup> or plasma, surface polymerization from a plasma polymer initiator layer,<sup>77</sup> atom transfer free radical polymerization,<sup>78</sup> iniferter polymerization, ionic polymerization, or photopolymerization. Other molecules similar to *N*-acryloylsarcosine methyl ester include *N*-methyl-*N*-2-propenyl methyl ester, acryloylsarcosine methyl ester,<sup>79</sup> *N*-methoxyethylglycine oligomers,<sup>80</sup> and related *N*-substituted glycine peptides. There also exists the scope for copolymerization or alternatively direct adsorption of *N*-substituted glycine derivative oligomers and polymers onto a solid substrate.

As well as being protein resistant, these surfaces could also be suitable for resistance toward cell adhesion, bacteria adhesion, and enzyme degradation. They could be employed for use in biomicro-electromechanical systems<sup>81</sup> and for other biomaterial surfaces where an immune response is not desired.

## 5. Conclusions

Pulsed plasmachemical deposition poly(*N*-acryloylsarcosine methyl ester) yields protein-resistant surfaces. This method has been successfully employed to coat a whole range of different substrate materials and geometries.

**Acknowledgment.** D. O. H. Teare thanks the Wellcome Trust for financial support, and J. P. S. Badyal is grateful to the EPSRC for an Advanced Research Fellowship.

## References and Notes

- (1) Brash, J. L.; Horbett, T. A. *ACS Symp. Ser.* **1995**, No. 602, 1.
- (2) Nakanishi, K.; Sakiyama, T.; Imamura, K. *J. Biosci. Bioeng.* **2001**, 91, 233.
- (3) Sun, Y. H.; Gombotz, W. R.; Hoffman, A. S. *J. Bioact. Compat. Polym.* **1986**, 1, 316.
- (4) Lee, J. H.; Kopeckova, P.; Zhang, J.; Kopecek, J.; Andrade, J. D. *Polym. Mater. Sci. Eng.* **1988**, 59, 234.
- (5) Lee, J. H.; Kopecek, J.; Andrade, J. D. *J. Biomed. Mater. Res.* **1989**, 23, 351.
- (6) Prime, K. L.; Whitesides, G. *Science* **1991**, 252, 1164.
- (7) Hayward, J. A.; Chapman, D. *Biomaterials* **1984**, 5, 135.
- (8) Ostuni, E.; Chapman, R. G.; Holmlin, R. E.; Takayama, S.; Whitesides, G. M. *Langmuir* **2001**, 17, 5605.
- (9) Ostuni, E.; Chapman, R. G.; Liang, M. N.; Meluleni, G.; Pier, G.; Ingber, D. R.; Whitesides, G. M. *Langmuir* **2001**, 17, 6336.

- (10) Chapman, R. G.; Ostuni, E.; Takayama, S.; Holmlin, R. E.; Yan, L.; Whitesides, G. M. *J. Am. Chem. Soc.* **2000**, *122*, 8303.
- (11) Kane, R. S.; Deschatelets, P.; Whitesides, G. M. *Langmuir* **2003**, *19*, 2388.
- (12) Luk, Y. Y.; Kato, M.; Mrksich, M. *Langmuir* **2000**, *16*, 9604.
- (13) Huber, D. L.; Manginell, R. P.; Samara, M. A.; Kim, B.; Bunker, B. C. *Science* **2003**, *301*, 352.
- (14) Wang, Y.; Cheng, X.; Hanein, Y.; Shastry, A.; Denton, D. D.; Ratner, B. D.; Bohringer, K. F. *Transducers '03 Int. Conf. Solid-State Sens. Actuators Microsyst., Dig. Tech Pap. 12 th* **2003**.
- (15) Chen, H.; Zhang, Z.; Chen, Y.; Brook, M. A.; Sheardown, H. *Biomaterials* **2005**, *26*, 2391.
- (16) Herrwerth, S.; Eck, W.; Reinhart, S.; Grunze, M. *J. Am. Chem. Soc.* **2003**, *125*, 9359.
- (17) Chapman, R. G.; Ostuni, E.; Liang, M. N.; Meluleni, G.; Kim, E.; Yan, L.; Pier, G.; Warren, H. S.; Whitesides, G. M. *Langmuir* **2001**, *17*, 1225.
- (18) Gu, J.; Yam, C. M.; Li, S.; Cai, C. *J. Am. Chem. Soc.* **2004**, *126*, 8098.
- (19) Jon, S.; Seong, J.; Khademhosseini, A.; Tran, T. N. T.; Laibinis, P. E.; Langer, R. *Langmuir* **2003**, *19*, 9989.
- (20) Lasseter, T. L.; Clare, B. H.; Abbott, N. L.; Hamers, R. J. *J. Am. Chem. Soc.* **2004**, *126*, 10220.
- (21) Groll, J.; Amirgoulova, E. V.; Ameringer, T.; Heyes, C. D.; Röcker, C.; Nienhaus, G. U.; Möller, M. *J. Am. Chem. Soc.* **2004**, *126*, 4234.
- (22) Nath, N.; Hyun, J.; Ma, H.; Chilkoti, A. *Surf. Sci.* **2004**, *570*, 98.
- (23) Chen, H.; Brook, M. A.; Sheardown, H. *Biomaterials* **2004**, *25*, 2273.
- (24) Frederix, F.; Bonroy, K.; Reekmans, G.; Laureyn, W.; Campitelli, A.; Abramov, M. A.; Dehaen, W.; Maes, G. *J. Biochem. Biophys. Methods* **2004**, *58*, 67.
- (25) Zhang, F.; Kang, E. T.; Neoh, K. G.; Wang, P.; Tan, K. L. *J. Biomed. Mater. Res.* **2001**, *56*, 324.
- (26) Kingshott, P.; Thissen, H.; Griesser, H. *J. Biomaterials* **2002**, *23*, 2043.
- (27) Zhang, Z.; Menges, B.; Timmons, R. B.; Knoll, W.; Förch, R. *Langmuir* **2003**, *19*, 4765.
- (28) Shen, M.; Wagner, M. S.; Castner, D. G.; Ratner, B. D.; Horbett, T. A. *Langmuir* **2003**, *19*, 1692.
- (29) Metzke, M.; Bai, J. Z.; Guan, Z. *J. Am. Chem. Soc.* **2003**, *125*, 7760.
- (30) Crouzet, C.; Decker, C.; Marchal, J. *Makromol. Chem.* **1976**, *177*, 145.
- (31) Branch, D. W.; Wheeler, B. C.; Brewer, G. J.; Leckband, D. E. *Biomaterials* **2001**, *22*, 1035.
- (32) Flynn, N. T.; Tran, T. N. T.; Cima, M. J.; Langer, R. *Langmuir* **2003**, *19*, 10909.
- (33) Lewis, A. L. *Colloids Surf., B* **2000**, *18*, 261.
- (34) Chapman, D. *Langmuir* **1993**, *9*, 39.
- (35) Ishihara, K.; Nomura, H.; Mihara, M.; Kurita, K.; Iwasaki, Y.; Nakabayashi, N. *J. Biomed. Mater. Res.* **1998**, *39*, 323.
- (36) Ross, E. E.; Spratt, T.; Liu, S.; Rozanski, L. J.; O'Brien, D. F.; Saavedra, S. S. *Langmuir* **2003**, *19*, 1766.
- (37) Malmsten, M. *J. Colloid Interface Sci.* **1995**, *172*, 106.
- (38) Malmsten, M. *Colloids Surf., A* **1999**, *159*, 77.
- (39) Glasmästar, K.; Larsson, C.; Höök, F.; Kasemo, B. *J. Colloid Interface Sci.* **2002**, *246*, 40.
- (40) Hsiue, G. H.; Lee, S. D.; Chang, P. C.; Kao, C. Y. *J. Biomed. Mater. Res.* **1998**, *42*, 134.
- (41) Holmlin, R. E.; Chen, X.; Chapman, R. G.; Takayama, S.; Whitesides, G. M. *Langmuir* **2001**, *17*, 2841.
- (42) West, S. L.; Salvage, J. P.; Lobb, E. J.; Armes, S. P.; Billingham, N. C.; Lewis, A. L.; Hanlon, G. W.; Lloyd, A. W. *Biomaterials* **2004**, *25*, 1195.
- (43) Massia, S. P.; Stark, J.; Letbetter, D. S. *Biomaterials* **2000**, *21*, 2253.
- (44) Holland, N. B.; Qiu, Y.; Ruegsegger, M.; Marchant, R. E. *Nature* **1998**, *392*, 799.
- (45) Griesser, H. J.; Hartley, P. G.; McArthur, S. L.; McLean, K. M.; Meagher, L.; Thissen, H. *Smart Mater. Struct.* **2002**, *11*, 652.
- (46) Duracher, D.; Veyret, R.; Elaissari, A.; Pichot, C. *Polym. Int.* **2004**, *53*, 618.
- (47) Deng, L.; Mrksich, M.; Whitesides, G. M. *J. Am. Chem. Soc.* **1996**, *118*, 5136.
- (48) Nath, N.; Chilkoti, A. *Anal. Chem.* **2003**, *75*, 709.
- (49) Kitano, H.; Kawasaki, A.; Kawasaki, H.; Morokoshi, S. *J. Colloid Interface Sci.* **2005**, *282*, 340.
- (50) Sweryda-Krawiec, B.; Devaraj, H.; Jacob, G.; Hickman, J. J. *Langmuir* **2004**, *20*, 2054.
- (51) Malmsten, M.; Muller, D.; Lassen, B. J. *Colloid Interface Sci.* **1997**, *193*, 88.
- (52) Vroman, L.; Adams, A. L.; Fischer, G. C.; Munoz, P. C. *Blood* **1980**, *55*, 156.
- (53) Statz, A. R.; Meagher, R. J.; Barron, A. E.; Messersmith, P. B. *J. Am. Chem. Soc.* **2005**, *127*, 7972.
- (54) Ryan, M. E.; Hynes, A. M.; Badyal, J. P. S. *Chem. Mater.* **1996**, *8*, 37.
- (55) Hutton, S. J.; Crowther, J. M.; Badyal, J. P. S. *Chem. Mater.* **2000**, *12*, 2282.
- (56) Tarducci, C.; Schofield, W. C. E.; Brewer, S. A.; Willis, C.; Badyal, J. P. S. *Chem. Mater.* **2001**, *13*, 1800.
- (57) Tarducci, C.; Kinmond, E. J.; Brewer, S. A.; Willis, C.; Badyal, J. P. S. *Chem. Mater.* **2000**, *12*, 1884.
- (58) Rinsch, C. L.; Chen, X. L.; Panchalingam, V.; Eberhart, R. C.; Wang, J. H.; Timmons, R. B. *Langmuir* **1996**, *12*, 2995.
- (59) Tarducci, C.; Brewer, S. A.; Willis, C.; Badyal, J. P. S. *Chem. Commun.* **2005**, *3*, 406.
- (60) Coulson, S. R.; Woodward, I. S.; Brewer, S. A.; Willis, C.; Badyal, J. P. S. *Chem. Mater.* **2000**, *12*, 2031.
- (61) Limb, S. J.; Gleason, K. K.; Edell, D. J.; Gleason, E. F. *J. Vac. Sci. Technol.* **1997**, *A15*, 1814.
- (62) Wang, J. H.; Chen, J. J.; Timmons, R. B. *Chem. Mater.* **1996**, *8*, 2212.
- (63) Tabet, F. M.; McGahan, W. A. *Thin Solid Films* **2000**, *370*, 122.
- (64) Evans, J. F.; Gibson, J. H.; Moulder, J. F.; Hammond, J. S.; Goretzki, H. *Fresenius J. Anal. Chem.* **1984**, *319*, 841.
- (65) Slack, S. M.; Bohnert, J. L.; Horbett, T. A. *Ann. N. Y. Acad. Sci.* **1987**, *516*, 223.
- (66) Kuehner, D. E.; Engmann, J.; Fergg, F.; Wernick, M.; Blanch, H. W.; Prausnitz, J. M. *J. Phys. Chem. B* **1999**, *103*, 1368.
- (67) Robeson, J. L.; Tilton, R. D. *Langmuir* **1996**, *12*, 6104.
- (68) Briggs, D.; Riviere, J. C. In *Practical Surface Analysis*, 2nd ed.; Briggs, D., Seah, M. P., Eds.; Wiley: Chichester, 1983; Volume 1.
- (69) Gouy, G. *J. Phys. Radium* **1910**, *9*, 457.
- (70) Chapman, D. L. *Philos. Mag.* **1913**, *25*, 475.
- (71) Rowe, A. J. *Biophys. Chem.* **2001**, *93*, 93.
- (72) Kitano, H.; Imai, M.; Sudo, K.; Ide, M. *J. Phys. Chem. B* **2002**, *106*, 11391.
- (73) Kitano, H.; Sudo, K.; Ichikawa, K.; Ide, M.; Ishihara, K. *J. Phys. Chem. B* **2000**, *104*, 11425.
- (74) Horbett, T. A.; Schway, M. B. *J. Biomed. Mater. Res.* **1988**, *22*, 763.
- (75) Ward, L. J. Internat. Patent. No. WO 03101621.
- (76) Akelah, A.; Heffernan, J. G.; Kingston, S. B.; Sherrington, D. C. *J. Appl. Polym. Sci.* **1983**, *28*, 3137.
- (77) Teare, D. O. H.; Schofield, W. C. E.; Roucoules, V.; Badyal, J. P. S. *Langmuir* **2003**, *19*, 2398.
- (78) Ayres, N.; Haddleton, D. M.; Shouter, A. J.; Pears, D. A. *Polym. Prepr.* **2001**, *42*, 514.
- (79) Kricheldorf, H. R.; Schilling, G. *Makromol. Chem.* **1977**, *178*, 3115.
- (80) Statz, A.; Meagher, R. J.; Barron, A. E.; Messersmith, P. B., Presented at the 2004 Fall Materials Research Society, Boston, MA, 2004.
- (81) Hanein, Y.; Pan, Y. V.; Ratner, B. D.; Denton, D. D.; Böhringer, K. F. *Sens. Actuators, B* **2001**, *81*, 49.